Table S1 Analytical methods, QC limits, and instrument provenance.

Parameter	Method	Instrument	S/N	LOD/LOQ	Calibration
COD	APHA 5220 D (closed reflux, dichromate) via Hach 10211	Hach DR6000 UV-Vis, λ = 620 nm, range 20-1,500 mg/L O_2	170904-0127	LOD 3 mg/L; LOQ 20 mg/L	2-pt factory + 500 mg/L KHP standard; blank <10 mg/L
BOD_5	APHA 5210 B (5-day, 20°C, dark incubation)	Hanna HI 9146 DO-meter; probe HI 76407	H9146/22-0371	LOD 2 mg/L	Air-saturated H_2O (100%), zero-O_2 (Na_2SO_3); ≤1.5% FS
TSS	APHA 2540 D (gravimetric, 103-105°C)	Sartorius MSA225S-100-DA (0.01 mg); oven Memmert UF-55	33070028	LOD 3 mg/L	Internal motorized cal., OIML F1 weights
pH	SNI 6989.11:2019	Hanna HI 2210	-	-	3-pt: 4.01, 7.01, 10.01
Conductivity	SNI 06-6989.1-2004	Hanna HI 98311	-	-	1,413 µS/cm KCl standard
Color	SNI 6989.80:2011 (Pt-Co, λ = 455 nm)	Hach DR6000	170904-0127	LOD 5 Pt-Co	Pt-Co standard series
Al dose verification	Gravimetric mass-loss	Sartorius MSA225S	33070028	-	OIML F1 weights

Calibration verification on 2025-08-21: - KHP 500 mg/L standard measured 498 mg/L (Δ = -0.4%, pass). - Duplicate precision on 300 mg/L standard: RPD 1.8% (pass < 5%). - Reagent blank: 2 mg/L (pass < 10 mg/L).

Table S2 Per-run voltage log.

Run	Spacing	t (min)	I (A)	$V_{readout}$ (V)	j (mA cm^{-2})	Per-run drift (mV)	Passivation observed?
1	4 cm	50	0.80	2.1	8	≤4	no
2	4 cm	75	1.00	2.3	10	≤4	no
3	4 cm	100	1.20	2.5	12	≤4	no
4	2 cm	50	1.20	1.8	12	≤4	no
5	2 cm	75	1.50	1.9	15	≤4	no
6	2 cm	100	1.80	2.0	18	≤4	no

Linear regression: 4 cm V = 0.100·j + 1.30 (R^2 = 1.000); 2 cm V = 0.033·j + 1.40 (R^2 = 1.000).

Table S3 Anode mass-loss validation (Run #1).

Measurement	Value
Pre-run plate mass	124.53 g
Post-run plate mass	124.34 g
Δm observed	**0.19 g**
Faraday prediction at ϕ = 0.92, I = 0.80 A, t = 50 min	0.206 g
Ratio observed/predicted	**0.92**

This direct empirical observation supports the ϕ = 0.92 assumption used throughout the kinetic and TEA framework.

Table S4 Candidate kinetic model forms. Six candidate kinetic forms were fitted to triplicate η-versus-Faraday-Al-dose data for each (parameter × spacing) combination (n = 9 observations). Model expressions (with η_{max} fixed at the literature asymptote 0.96/0.95/0.99 for COD/BOD_5/TSS):

Model	Expression	Free parameters
Exponential saturation	$\eta = \eta_{max} \cdot [1 - \exp(-k \cdot C)]$	k
PFO (Lagergren)	$\eta = \eta_{max} \cdot [1 - \exp(-k_1 \cdot C)]$	k_1
PSO (Ho & McKay)	$\eta = \eta_{max}^2 \cdot k_2 \cdot C/(1 + \eta_{max} \cdot k_2 \cdot C)$	k_2
Langmuir-hyperbolic	$\eta = \eta_{max} \cdot C/(K + C)$	K
Gompertz	$\eta = \eta_{max} \cdot \exp(-\exp(-k_g \cdot (C - C_{lag})))$	k_g, C_{lag}
Logistic	$\eta = \eta_{max}/(1 + \exp(-k_l \cdot (C - C_{50})))$	k_l, C_{50}

Note: PFO and exponential saturation are functionally identical when C_{Al} serves as the integrated dose variable; their AIC values coincide by construction.

Table S5 Model comparison per (parameter × spacing). The full AIC, BIC, R^2, and parameter estimates for all 36 model fits (6 parameters × 6 model types) are in the accompanying analysis bundle. Headline ΔAIC ranking:

Parameter	Spacing	Best model	R^2 best	ΔAIC over exp. sat.
COD	4 cm	Gompertz	0.994	+5.2
COD	2 cm	Logistic	0.960	+6.3
BOD_5	4 cm	Gompertz	0.971	+9.9
BOD_5	2 cm	Logistic	0.967	+12.7
TSS	4 cm	Gompertz	0.997	+38.3
TSS	2 cm	Logistic	0.982	+17.5

Table S6 Bootstrap 95% confidence intervals for rate constant k. Pairs bootstrap with n_{boot} = 10,000 resamples, drawn from the full 9-observation triplicate dataset per (parameter × spacing). All bootstrap CIs are strictly positive.

Parameter	Gap	Data pts	k_{point} (L/mg)	$k_{boot\ mean}$	$k_{boot\ SD}$	95% CI (lo)	95% CI (hi)
COD	4 cm	9	0.00346	0.00346	0.00007	0.00332	0.00358
COD	2 cm	9	0.00459	0.00461	0.00024	0.00421	0.00518
BOD_5	4 cm	9	0.00264	0.00262	0.00018	0.00223	0.00294
BOD_5	2 cm	9	0.00410	0.00412	0.00031	0.00363	0.00483
TSS	4 cm	9	0.00171	0.00167	0.00028	0.00105	0.00215
TSS	2 cm	9	0.00416	0.00418	0.00033	0.00363	0.00490

Key improvement: For TSS/4 cm, the asymptotic Wald CI [-0.00083, +0.00424] crossed zero, but the bootstrap CI [0.00105, 0.00215] is strictly positive, confirming that k is statistically distinguishable from zero.

To test whether the two-way ANOVA on η is reducible to a single "total charge Q" effect, Type-II ANCOVA was performed with plate spacing as a categorical factor and Q (Coulombs) as a continuous covariate. The interaction term (spacing × Q) tests whether the η-versus-Q slope differs between gaps.

Table S7 ANCOVA with total charge Q as covariate - spacing main-effect model.

Parameter	Model	R^2	AIC
COD	spacing + Q	0.991	-127.8
COD	spacing + Q + spacing × Q	0.992	-127.6
BOD_5	spacing + Q	0.965	-95.0
TSS	spacing + Q	0.991	-113.0

ANCOVA results for the spacing main effect after controlling for Q:

Table S8 ANCOVA F-test for the spacing × Q interaction.

Parameter	F (df)	p-value
COD	23.2 (1, 50)	4.4×10^{-5}
BOD_5	24.0 (1, 50)	3.8×10^{-5}
TSS	56.7 (1, 50)	2.0×10^{-8}

The spacing × Q interaction (different η-versus-Q slopes per gap) is also significant for COD ($p < 10^{-3}$) and TSS ($p < 10^{-4}$).

Interpretation. The two-way ANOVA captures a real geometric/mass-transfer effect of plate spacing beyond the coulombic load; the original interaction interpretation in §3.2 is therefore not an artifact of confounded variables.

Table S9 Model comparison: exponential-saturation vs Langmuir (AIC/BIC). Both models have 1 free parameter (k for exponential; K for Langmuir); η_{max} is fixed from the literature. Negative ΔAIC favors exponential-saturation.

Parameter	Gap	exp k (L/mg)	exp R^2	exp AIC	Langmuir K (mg/L)	Lang R^2	Lang AIC	ΔAIC	Preferred
COD	4 cm	0.00346	0.990	-69.72	204	0.915	-51.50	-18.22	exp-sat (decisive)
COD	2 cm	0.00459	0.914	-50.02	139	0.835	-38.72	-11.30	exp-sat (decisive)
BOD_5	4 cm	0.00264	0.911	-48.68	340	0.748	-42.94	-5.74	exp-sat (substantial)
BOD_5	2 cm	0.00410	0.876	-44.15	170	0.740	-35.07	-9.08	exp-sat (decisive)
TSS	4 cm	0.00171	0.696	-36.57	658	0.711	-34.61	-1.96	exp-sat (weak)
TSS	2 cm	0.00416	0.866	-41.82	175	0.700	-32.90	-8.92	exp-sat (decisive)

ΔAIC interpretation [1]: |Δ| > 10 decisive; 4-7 substantial; 2-4 weak.

Table S10 Analytical QC summary.

Analyte	QC item	Value	APHA threshold	Pass
COD	Calibration check (KHP 500 mg L^{-1})	498 mg L^{-1} (-0.4%)	±5%	✓
COD	Pre-run blank	3.2 mg L^{-1}	≤10 mg L^{-1}	✓
COD	Post-run blank	1.5 mg L^{-1}	≤10 mg L^{-1}	✓
COD	Std-recovery (KHP 500 mg L^{-1})	98.5%	90-110%	✓
COD	Duplicate 300 mg L^{-1} std	RPD 1.8%	<5%	✓
COD	Duplicate sample (4 cm/50 min/R1)	RPD 1.5%	<5%	✓
COD	Method RSD (n = 3 std at 300 mg L^{-1})	3.3%	matches APHA spec	✓
BOD_5	Dilution-water blank	0.35 mg L^{-1}	≤0.6 mg L^{-1}	✓
BOD_5	ΔDO range (all samples)	2.0-6.0 mg L^{-1}	APHA range	✓
TSS	Gravimetric duplicate (a)	RPD 1.2%	<5%	✓
TSS	Gravimetric duplicate (b)	RPD 2.8%	<5%	✓

All 11 QC indicators passed APHA thresholds.

Table S11 Justification of TEA variation ranges.

Parameter	Base value	Range	Source category	Rationale
Kinetic rate constant k_{COD} (at 2 cm)	0.00459 L mg^{-1}	± 30%	experimental	Bootstrap CI (± 10%) + between-spacing range (± 14%)
Aluminum plate price	IDR 40,000 kg^{-1}	± 30%	market	Indonesian B2B supplier quotes 2024 (IDR 28,000-52,000 kg^{-1})
Operational current density j^*	1.5 mA cm^{-2}	± 20%	experimental	§3.7 Monte Carlo 95% CI (1.25-1.78 mA cm^{-2})
Faraday efficiency ϕ	0.92	0.85-0.95	literature	EC textile reviews [2, 3]
Electricity tariff	IDR 1,035.78 kWh^{-1}	± 10%	regulatory	PLN industrial-tariff bulletins 2020-2024

Methodology Declaration

- **Cut-off (ISO 14044 recycled-content method):** primary-Al producer carries 100% of upstream impacts; recycled Al pays only re-melting (≈1.2 kg CO_2 kg^{-1}). Sludge: no credit. *Baseline for headline figures because it is the most conservative for recycled-electrode scenarios.*
- **Avoided burden:** sludge that displaces primary alum downstream earns a credit equal to $EF_{alum} \times m_{sludge,\ alum\text{-}equivalent}$. Sludge efficacy as a secondary coagulant is set conservatively at 60% of primary alum (literature 0.55-0.75). *Reported for transparency only; not used as a basis for a sustainability claim.*
- **50:50 allocation:** recycled-Al upstream burden split evenly between first and second life.

Table S12 Full 3 × 2 × 2 carbon-footprint scenario matrix.

Allocation	Electrode	Energy	$CO_{2,\ energy}$	$CO_{2,\ electrode}$	$CO_{2,\ gross}$	Credit	$CO_{2,\ net}$ (kg m^{-3})
Cut-off	Primary	Grid	1.13	9.24	10.37	0.00	**10.37**
Cut-off	Primary	PV	0.07	9.24	9.30	0.00	9.30
Cut-off	Recycled	Grid	1.13	0.92	2.05	0.00	**2.05**
Cut-off	Recycled	PV	0.07	0.92	0.99	0.00	**0.99**
Avoided	Primary	Grid	1.13	9.24	10.37	2.54	7.83
Avoided	Primary	PV	0.07	9.24	9.30	2.54	6.77
Avoided	Recycled	Grid	1.13	0.92	2.05	2.54	-0.48
Avoided	Recycled	PV	0.07	0.92	0.99	2.54	-1.55
50:50	Primary	Grid	1.13	9.24	10.37	0.00	10.37
50:50	Primary	PV	0.07	9.24	9.30	0.00	9.30
50:50	Recycled	Grid	1.13	5.08	6.21	0.00	6.21
50:50	Recycled	PV	0.07	5.08	5.15	0.00	5.15

Table S13 Triplicate statistics for all 18 batch runs. Quality-control summary: means, standard deviations, coefficients of variation, Grubbs statistics ($G_{0.05,\,3}$ = 1.1543), observed removal efficiencies, and regulatory compliance.

Parameter	Gap (cm)	Time (min)	C_{Al} (mg/L)	Rep 1	Rep 2	Rep 3	Mean (mg/L)	SD (mg/L)	CV (%)	Range	Grubbs G	Outlier	η (%)	PermenLHK limit (mg/L)	Compliance
COD	4	50	102.9	532	553	552	545.67	11.85	2.17	21	1.154	No	27.24	100	No
COD	4	75	192.9	418	393	407	406.00	12.53	3.09	25	1.038	No	45.87	100	No
COD	4	100	308.7	266	261	262	263.00	2.65	1.01	5	1.134	No	64.93	100	No
COD	2	50	154.4	396	404	391	397.00	6.56	1.65	13	1.067	No	47.07	100	No
COD	2	75	289.4	253	262	247	254.00	7.55	2.97	15	1.060	No	66.13	100	No
COD	2	100	463.1	50	56	55	53.67	3.21	5.99	6	1.141	No	92.84	100	**Yes**
BOD_5	4	50	102.9	255	271	278	268.00	11.79	4.40	23	1.103	No	16.25	50	No
BOD_5	4	75	192.9	189	218	214	207.00	15.72	7.59	29	1.145	No	35.31	50	No
BOD_5	4	100	308.7	137	127	132	132.00	5.00	3.79	10	1.000	No	58.75	50	No
BOD_5	2	50	154.4	189	195	199	194.33	5.03	2.59	10	1.060	No	39.27	50	No
BOD_5	2	75	289.4	127	120	119	122.00	4.36	3.57	8	1.147	No	61.88	50	No
BOD_5	2	100	463.1	23.2	24.8	27.2	25.07	2.01	8.03	4	1.060	No	92.17	50	**Yes**
TSS	4	50	102.9	660	676	673	669.67	8.50	1.27	16	1.137	No	1.52	50	No
TSS	4	75	192.9	555	528	535	539.33	14.01	2.60	27	1.118	No	20.69	50	No
TSS	4	100	308.7	329	314	320	321.00	7.55	2.35	15	1.060	No	52.79	50	No
TSS	2	50	154.4	425	411	417	417.67	7.02	1.68	14	1.044	No	38.58	50	No
TSS	2	75	289.4	226	222	218	222.00	4.00	1.80	8	1.000	No	67.35	50	No
TSS	2	100	463.1	22.2	19.1	18.4	19.90	2.02	10.16	4	1.137	No	97.07	50	**Yes**

Acceptance criteria: - APHA method precision: COD ± 3.3%, BOD_5 ± 6.5%, TSS ± 4.2%. All CVs within or close to these bounds; BOD_5 slightly higher for 4 cm/50 min (CV 4.4%), acceptable given low dose regime. - Grubbs two-sided critical value at α = 0.05, n = 3 is 1.1543. All measured G values ≤ 1.154 → no significant outliers.

Table S14 Extended EC-literature comparator (textile/batik scope). The main-text Table 8 retains the non-textile comparators [4, 5] as order-of-magnitude operating-cost benchmarks only, with explicit clarification in §3.11; this SI version reproduces the same textile and batik effluent comparator rows from main-text Table 8, kept as a standalone reference for readers who want the kinetic comparison without the food-processing comparators.

Reference	Wastewater	Mode	Electrode	COD η (%)	j (mA cm^{-2})	E (kWh m^{-3})	Cost (USD m^{-3})
Bener et al. [6]	Real textile	Batch	Fe	18.6	20	N/R	1.50
Bazrafshan et al. [7]	Textile	Batch	Al	72	40	N/R	N/R
Fadzli et al. [8]	Batik	Batch	Al/Fe	60-85	10-25	N/R	N/R
Lamhar et al. [9]	Synthetic textile	Continuous	Al	70-90 colour	5-12	2.0-6.5	N/R
Agarwal et al. [10]	Textile	Batch (novel reactor)	Al	75-92	10-30	2.5-5.0	N/R
Cruz et al. [11]	Textile (Remazol Red)	Batch	Al/Fe	85-96	15-25	4.5	2.10
Rezaei et al. [12]	Real dyeing	Batch (novel)	Al/Fe	83	15	N/R	N/R
This study (lab-batch optimum)	**Real batik cap**	**Batch**	**Al**	**92.8**	**18**	**3.4 (system)**	**0.94**
This study (continuous projection)	**Real batik cap**	**Continuous (model)**	**Al**	**99.7†**	**1.4**	**2.7 (system)**	**1.34 (approx. CI 1.05-1.75)**

† Cumulative for dual-EC + FRP filter; predictive (not yet validated). N/R = not reported. The two non-textile comparators that appear in main-text Table 8 ([4] on coffee; [5] on slaughterhouse) are excluded from this SI version because their dye chemistry differs substantially from batik; they are retained in main-text Table 8 only as order-of-magnitude operating-cost benchmarks, with the limitation stated explicitly in §3.11.

Table S15 Complete Tukey HSD pairwise comparison. Significance threshold α = 0.05. "reject = True" means the pair is significantly different.

Parameter	Group 1	Group 2	Mean diff (mg/L)	p-adj	95% CI lower	95% CI upper	Significant
COD	2 cm, 100 min	2 cm, 50 min	343.33	0.000	320.53	366.13	Yes
COD	2 cm, 100 min	2 cm, 75 min	200.33	0.000	177.53	223.13	Yes
COD	2 cm, 100 min	4 cm, 100 min	209.33	0.000	186.53	232.13	Yes
COD	2 cm, 100 min	4 cm, 50 min	492.00	0.000	469.20	514.80	Yes
COD	2 cm, 100 min	4 cm, 75 min	352.33	0.000	329.53	375.13	Yes
COD	2 cm, 50 min	2 cm, 75 min	-143.00	0.000	-165.80	-120.20	Yes
COD	2 cm, 50 min	4 cm, 100 min	-134.00	0.000	-156.80	-111.20	Yes
COD	2 cm, 50 min	4 cm, 50 min	148.67	0.000	125.87	171.47	Yes
COD	2 cm, 50 min	4 cm, 75 min	9.00	0.767	-13.80	31.80	**No**
COD	2 cm, 75 min	4 cm, 100 min	9.00	0.767	-13.80	31.80	**No**
COD	2 cm, 75 min	4 cm, 50 min	291.67	0.000	268.87	314.47	Yes
COD	2 cm, 75 min	4 cm, 75 min	152.00	0.000	129.20	174.80	Yes
COD	4 cm, 100 min	4 cm, 50 min	282.67	0.000	259.87	305.47	Yes
COD	4 cm, 100 min	4 cm, 75 min	143.00	0.000	120.20	165.80	Yes
COD	4 cm, 50 min	4 cm, 75 min	-139.67	0.000	-162.47	-116.87	Yes
BOD_5	2 cm, 100 min	2 cm, 50 min	169.27	0.000	145.27	193.26	Yes
BOD_5	2 cm, 100 min	2 cm, 75 min	96.93	0.000	72.94	120.93	Yes
BOD_5	2 cm, 100 min	4 cm, 100 min	106.93	0.000	82.94	130.93	Yes
BOD_5	2 cm, 100 min	4 cm, 50 min	242.93	0.000	218.94	266.93	Yes
BOD_5	2 cm, 100 min	4 cm, 75 min	181.93	0.000	157.94	205.93	Yes
BOD_5	2 cm, 50 min	2 cm, 75 min	-72.33	0.000	-96.33	-48.34	Yes
BOD_5	2 cm, 50 min	4 cm, 100 min	-62.33	0.000	-86.33	-38.34	Yes
BOD_5	2 cm, 50 min	4 cm, 50 min	73.67	0.000	49.67	97.66	Yes
BOD_5	2 cm, 50 min	4 cm, 75 min	12.67	0.515	-11.33	36.66	**No**
BOD_5	2 cm, 75 min	4 cm, 100 min	10.00	0.727	-14.00	34.00	**No**
BOD_5	2 cm, 75 min	4 cm, 50 min	146.00	0.000	122.00	170.00	Yes
BOD_5	2 cm, 75 min	4 cm, 75 min	85.00	0.000	61.00	109.00	Yes
BOD_5	4 cm, 100 min	4 cm, 50 min	136.00	0.000	112.00	160.00	Yes
BOD_5	4 cm, 100 min	4 cm, 75 min	75.00	0.000	51.00	99.00	Yes
BOD_5	4 cm, 50 min	4 cm, 75 min	-61.00	0.000	-85.00	-37.00	Yes
TSS	2 cm, 100 min	2 cm, 50 min	397.77	0.000	375.51	420.02	Yes
TSS	2 cm, 100 min	2 cm, 75 min	202.10	0.000	179.85	224.35	Yes
TSS	2 cm, 100 min	4 cm, 100 min	301.10	0.000	278.85	323.35	Yes
TSS	2 cm, 100 min	4 cm, 50 min	649.77	0.000	627.51	672.02	Yes
TSS	2 cm, 100 min	4 cm, 75 min	519.43	0.000	497.18	541.69	Yes
TSS	2 cm, 50 min	2 cm, 75 min	-195.67	0.000	-217.92	-173.41	Yes
TSS	2 cm, 50 min	4 cm, 100 min	-96.67	0.000	-118.92	-74.41	Yes
TSS	2 cm, 50 min	4 cm, 50 min	252.00	0.000	229.75	274.25	Yes
TSS	2 cm, 50 min	4 cm, 75 min	121.67	0.000	99.41	143.92	Yes

TSS	2 cm, 75 min	4 cm, 100 min	99.00	0.000	76.75	121.25	Yes
TSS	2 cm, 75 min	4 cm, 50 min	447.67	0.000	425.41	469.92	Yes
TSS	2 cm, 75 min	4 cm, 75 min	317.33	0.000	295.08	339.59	Yes
TSS	4 cm, 100 min	4 cm, 50 min	348.67	0.000	326.41	370.92	Yes
TSS	4 cm, 100 min	4 cm, 75 min	218.33	0.000	196.08	240.59	Yes
TSS	4 cm, 50 min	4 cm, 75 min	-130.33	0.000	-152.59	-108.08	Yes

Key non-significant pairs (trade-off spacing vs. time): - COD: (2 cm, 50 min) ≈ (4 cm, 75 min), p = 0.77 - COD: (2 cm, 75 min) ≈ (4 cm, 100 min), p = 0.77 - BOD_5: (2 cm, 50 min) ≈ (4 cm, 75 min), p = 0.52 - BOD_5: (2 cm, 75 min) ≈ (4 cm, 100 min), p = 0.73.

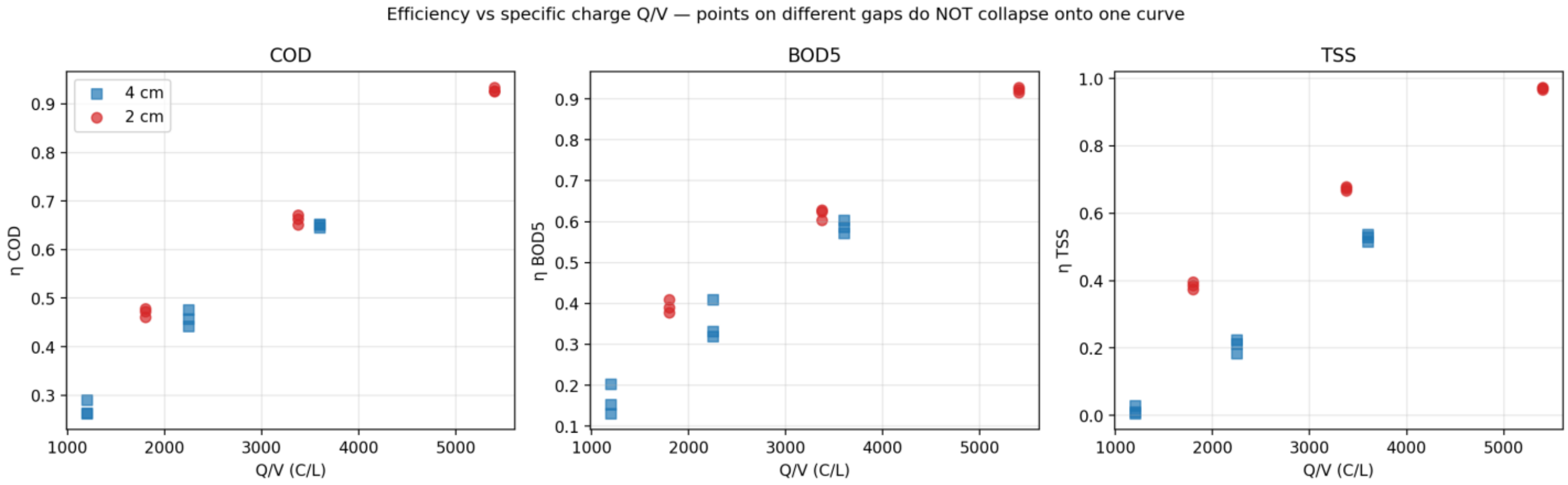

Figure S1 η versus specific charge Q/V (collapse test). Three-panel scatter of η versus specific charge Q/V (C L^{-1}), one panel per pollutant, with separate symbols for 4 cm and 2 cm gap. The series does not collapse onto a single curve at equal Q/V, providing visual confirmation of the ANCOVA result.

Table S16 Residual standard deviation versus APHA method precision.

Parameter	Mean effluent (mg L^{-1})	APHA-implied SD (mg L^{-1})	Observed residual SD (mg L^{-1})	Ratio observed/APHA
COD	327.0	10.8	8.5	0.79
BOD_5	165.0	10.7	9.1	0.85
TSS	365.0	15.3	8.1	0.53

All ratios ≤1.0, indicating residual variance is consistent with - not below - APHA-published analytical precision. Argument: residual variance is therefore *not artificially constrained*.

Table S17 Bootstrap 95% CIs for partial η^2. Pairs-resampling, n_{boot} = 2000:

Parameter	$\eta^2_{spacing}$ (95% CI)	η^2_{time} (95% CI)	$\eta^2_{interaction}$ (95% CI)
COD	0.994 (0.983-0.999)	0.997 (0.996-1.000)	0.838 (0.288-0.997)
BOD_5	0.953 (0.633-0.998)	0.979 (0.965-0.998)	0.635 (0.107-0.989)
TSS	0.978 (0.973-1.000)	0.998 (0.989-1.000)	0.868 (0.443-0.999)

All main-effect η^2 95% CIs are entirely above Cohen's “large” threshold (0.14), by a margin of more than 0.6.

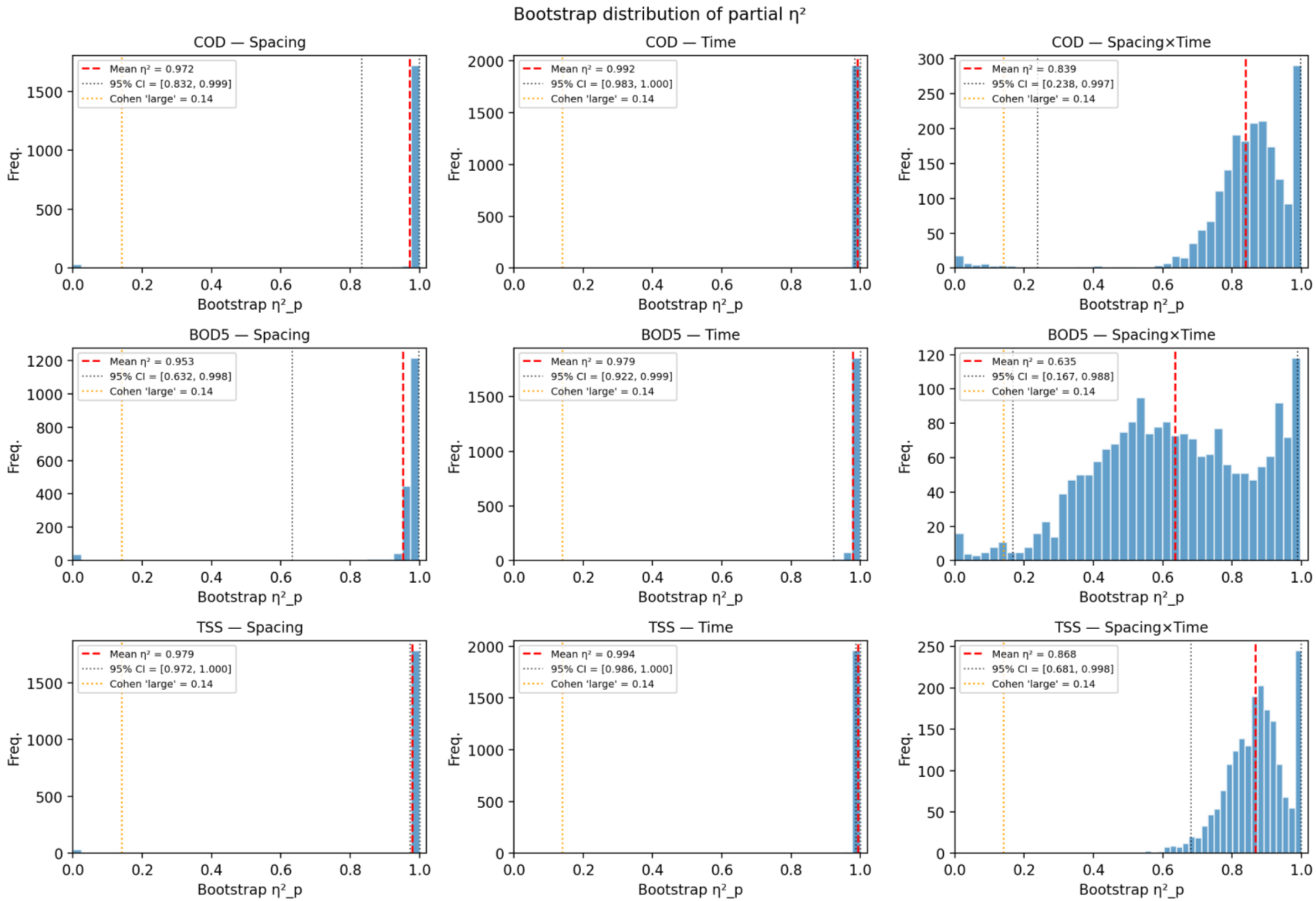

Figure S2 Bootstrap distribution of partial η^2. Nine-panel histogram of bootstrapped η^2_p with mean (red dashed), 95% CI (black dotted), and Cohen's "large" reference (orange dotted).

Table S18 Faraday theoretical dose and energy balance.

Gap	t (min)	j (mA/cm^2)	I (A)	Q (C)	Q/V (C/L)	Moles Al	m_{Al} Faraday (g)	C_{Al} (mg/L)	E_{theor} (kWh/m^3)	$E_{measured}$ (kWh/m^3)	ΔE (%)
4 cm	50	8	0.80	2,400	1,200	0.0076	0.206	102.9	0.67	1.2	+79
4 cm	75	10	1.00	4,500	2,250	0.0143	0.386	192.9	1.25	1.8	+44
4 cm	100	12	1.20	7,200	3,600	0.0229	0.617	308.7	2.00	2.4	+20
2 cm	50	12	1.20	3,600	1,800	0.0114	0.309	154.4	1.00	1.6	+60
2 cm	75	15	1.50	6,750	3,375	0.0215	0.579	289.4	1.88	2.3	+22
2 cm	100	18	1.80	10,800	5,400	0.0343	0.926	463.1	3.00	3.1	+3

$\Delta E = (E_{measured} - E_{theor})/E_{theor} \times 100\%$. Overhead decreases at high current because line and load-regulation losses become a smaller fraction of total power.

Table S19 Stoichiometric sludge mass balance ($Al \rightarrow Al(OH)_3$). Stoichiometric conversion: $m_{Al}(OH)_3 = m_{Al} \times (78/27) = 2.889 \times m_{Al}$. Wet-sludge volume assumes 2.5% solids content (typical for $Al(OH)_3$ sludge without thickening).

Gap	t (min)	j (mA/cm^2)	C_{Al} (mg/L)	m_{Al} per m^3 (g)	$m_{Al}(OH)_3$ per m^3 (g)	Dry sludge (kg/m^3)	Wet sludge (L/m^3)
4 cm	50	8	102.9	103	298	0.30	11.9
4 cm	75	10	192.9	193	558	0.56	22.3
4 cm	100	12	308.7	309	892	0.89	35.7
2 cm	50	12	154.4	154	447	0.45	17.9
2 cm	75	15	289.4	289	837	0.84	33.5
2 cm	100	18	463.1	463	1,338	1.34	53.5

Projected full-plant wet sludge at operational $j^* = 1.5$ mA/cm^2, Q = 1 m^3/day, dual-chamber series: ≈60 L/day. This is a key sizing parameter for sludge storage and periodic off-take logistics.

Table S20 Residual diagnostics of kinetic fit. Representative residuals ($\eta_{observed} - \eta_{predicted}$) for all 18 triplicate observations (9 per spacing). Residuals were pooled across (parameter × spacing) combinations for Shapiro-Wilk normality testing.

Parameter	Gap	Shapiro-Wilk W	p-value	Normality OK (α = 0.05)
COD	4 cm	0.933	0.510	Yes
COD	2 cm	0.957	0.771	Yes
BOD_5	4 cm	0.978	0.946	Yes
BOD_5	2 cm	0.921	0.399	Yes
TSS	4 cm	0.849	0.076	Yes
TSS	2 cm	0.943	0.615	Yes

The full per-observation residual table is provided in the analysis bundle. Diagnostics visual: residuals vs. C_{Al} and QQ-plots (Figure S3).

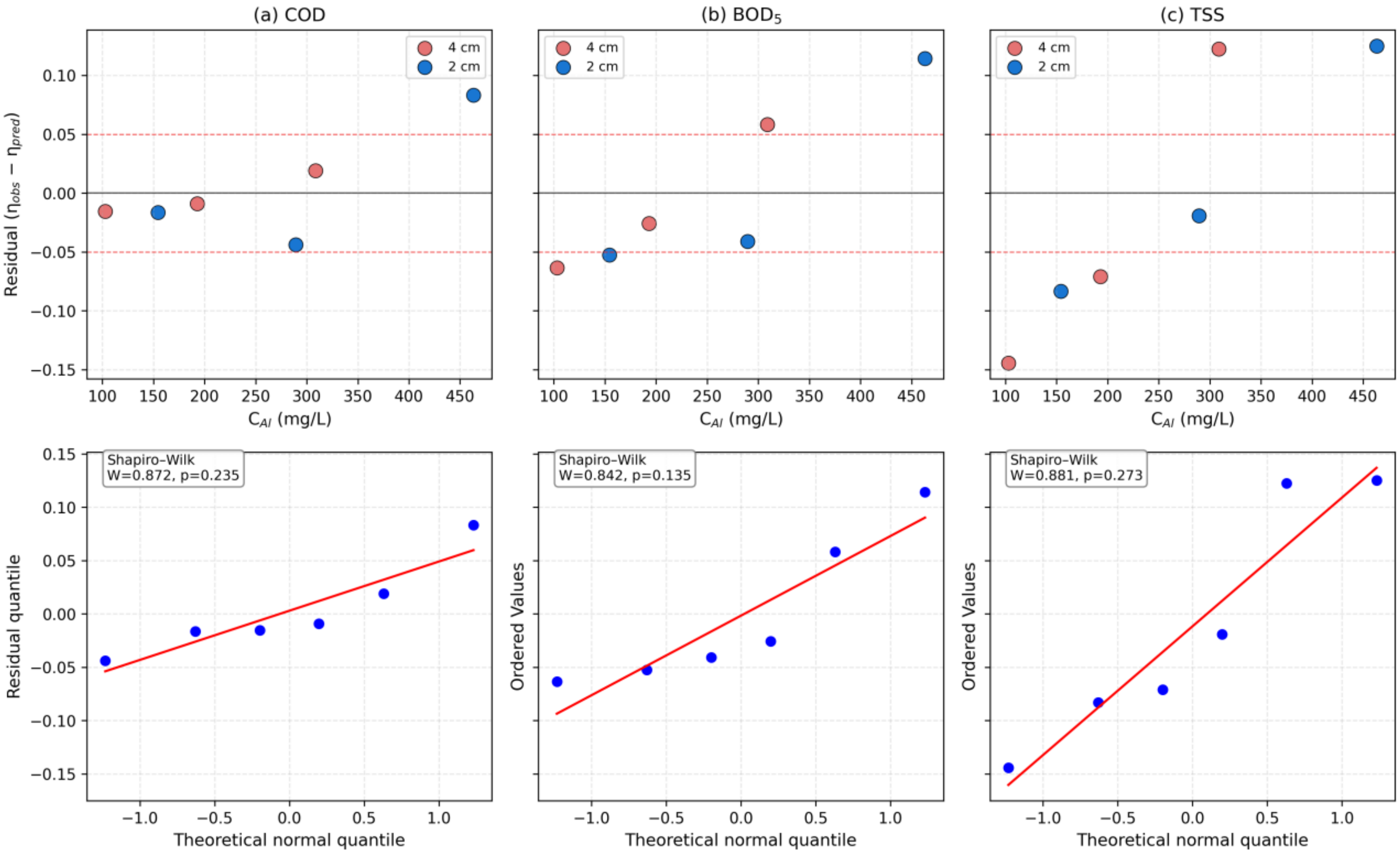

Figure S3 Residual diagnostics for the kinetic fit. Top row: residuals versus C_{Al} for each parameter and spacing. Bottom row: QQ-plots of residuals against theoretical normal quantiles, with Shapiro-Wilk statistics reported in the panel.

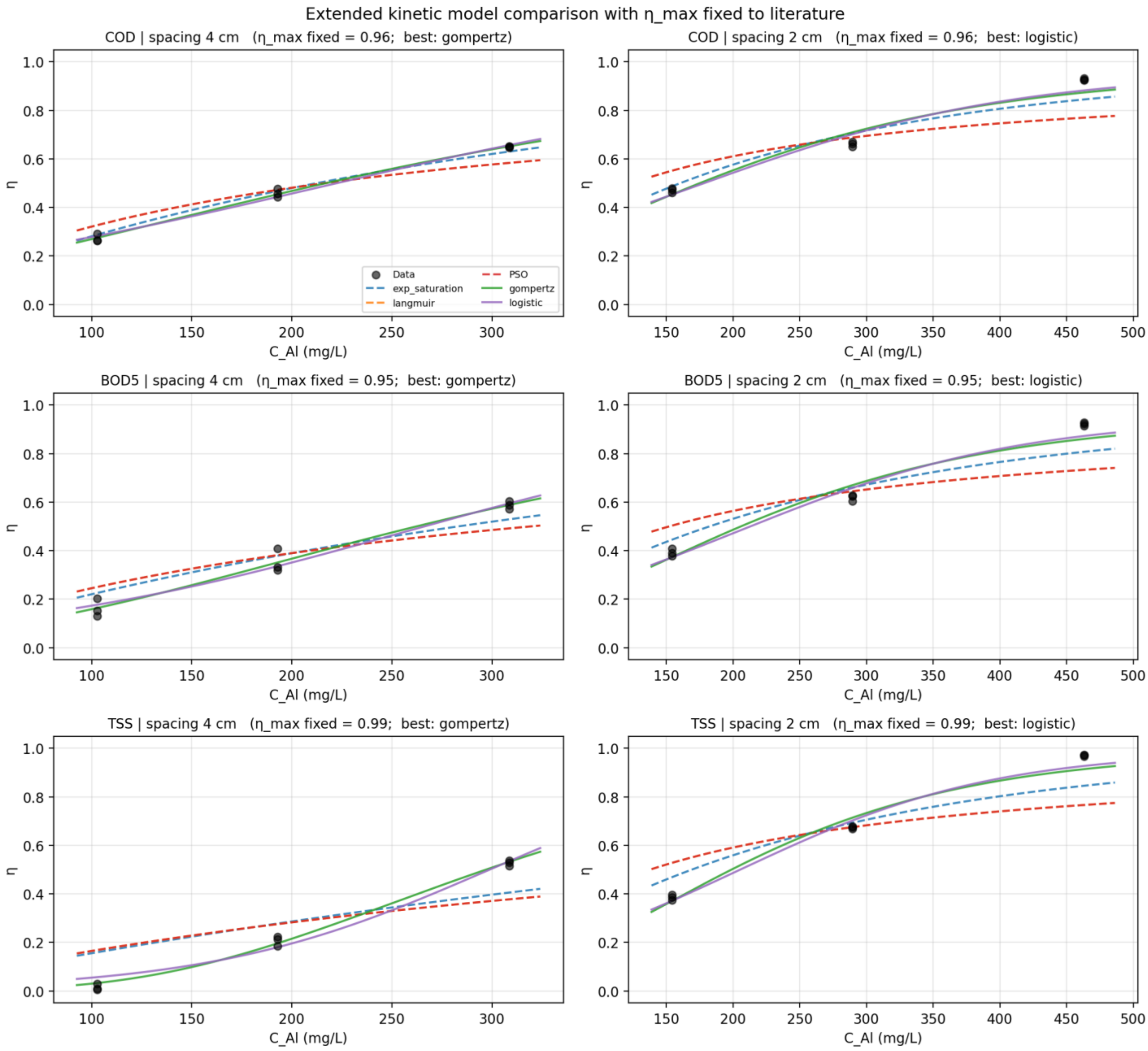

Figure S4 Kinetic model overlay. Six-panel overlay of all six fits per (parameter × spacing) condition, with triplicate data points. Best-fit model is named in each panel title.

Table S21 Holt [2] spacing-factor test. Holt's framework predicts k ∝ 1/d for the IR-drop-limited regime. Theoretical ratio k_2/k_4 = 4/2 = 2.0 (exact).

Parameter	k_4 cm	k_2 cm	Observed ratio	Theoretical (IR)	Deviation	Regime interpretation
COD	0.00346	0.00459	1.32	2.00	-34%	Chemistry-limited (dye adsorption kinetics dominate over ohmic)
BOD_5	0.00264	0.00410	1.55	2.00	-22%	Chemistry-limited (biodegradable-organic adsorption)
TSS	0.00171	0.00416	2.44	2.00	+22%	Mass-transfer-enhanced (floc-H_2 flotation boost in narrow gap)

Physical interpretation. For pure IR-limited electrocoagulation, halving the inter-plate gap doubles k. Our organic-related parameters (COD, BOD_5) give ratios <2, indicating that ohmic resistance is *not* the rate-limiting step - dye/organic adsorption kinetics on $Al(OH)_3$ flocs dominate. TSS exceeds 2.0, consistent with enhanced floc-gas agglomerate flotation in the narrow chamber. This regime classification justifies why operational j^* for continuous-flow can be an order of magnitude below the experimental batch range: pushing j beyond the chemistry-limited plateau gives no additional removal.

Per-condition sludge mass and disposal cost are tabulated for each (spacing × detention-time) condition. Calculations use the over-Faradaic factor f_{OF} = 1.30, an assumed 2.5% wet-solids content for unthickened $Al(OH)_3$, and a permitted off-site B3 disposal tariff of IDR 50/L of wet sludge.

Table S22 Per-condition sludge mass and disposal cost.

Spacing	t (min)	j (mA/cm^2)	Al actual (g/m^3)	Dry sludge (kg/m^3)	Wet sludge (L/m^3)	Disposal (IDR/m^3)	Disposal (USD/m^3)
2 cm	50	12	200.8	0.580	23.2	1161	0.073
2 cm	75	15	376.4	1.088	43.5	2175	0.136
2 cm	100	18	601.9	1.739	69.6	3479	0.217
4 cm	50	8	133.9	0.387	15.5	774	0.048
4 cm	75	10	250.9	0.725	29.0	1450	0.091
4 cm	100	12	401.1	1.159	46.4	2318	0.145

Table S23 Sludge productivity index (g pollutant removed per g dry sludge).

Spacing	t (min)	SPI_{COD}	SPI_{BOD5}	SPI_{TSS}
2 cm	50	0.608	0.217	0.452
2 cm	75	0.456	0.182	0.421
2 cm	100	0.400	0.170	0.379
4 cm	50	0.528	0.134	0.027
4 cm	75	0.474	0.156	0.194
4 cm	100	0.420	0.162	0.310

Table S24 Marginal sludge cost (kg dry sludge per percentage-point η gain). Computed within each spacing as Δsludge/Δη over the time series; values are absolute.

Spacing	t (min)	$\Delta sludge/\Delta pp_{COD}$	$\Delta sludge/\Delta pp_{BOD5}$	$\Delta sludge/\Delta pp_{TSS}$
2 cm	50	-	-	-
2 cm	75	0.0266	0.0224	0.0176
2 cm	100	0.0244	0.0215	0.0219
4 cm	50	-	-	-
4 cm	75	0.0182	0.0177	0.0176
4 cm	100	0.0228	0.0185	0.0135

Key observations:

- The highest sludge-productivity index (SPI_{COD} = 0.61 g COD g^{-1} dry sludge) is observed at 2 cm/50 min; lower-dose conditions are inherently more sludge-efficient on a pollutant-mass basis but do not meet discharge limits.
- The laboratory optimum (2 cm/100 min, j = 18 mA cm^{-2}) produces approximately 1.74 kg dry sludge m^{-3} (≈70 L wet sludge m^{-3} at 2.5% solids) - the highest sludge volume of all six conditions and the primary consideration for MSME deployment.
- The marginal sludge cost rises steeply as η approaches the asymptote, providing operators with a quantitative trade-off lever between effluent quality and sludge logistics.

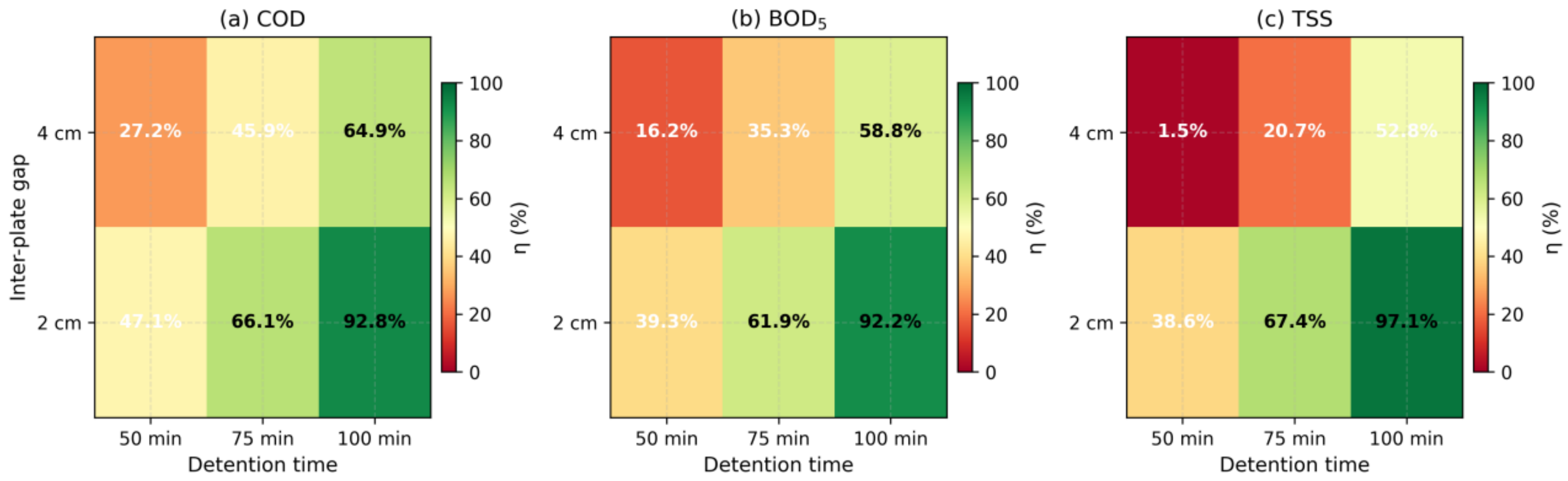

Figure S5 Factorial heat-map of removal efficiency across the 2 × 3 design (inter-plate gap × detention time) for COD, BOD_5, and TSS. Values in cells indicate η (%).

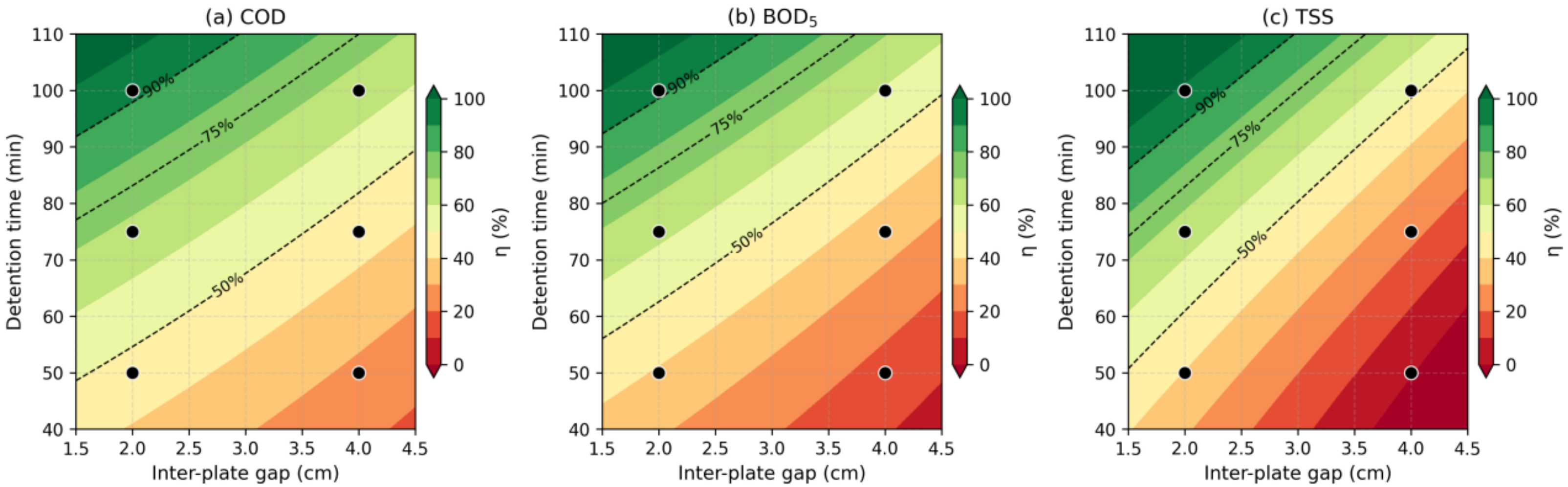

Figure S6 Second-order response-surface contour of removal efficiency across the continuous (inter-plate gap, detention time) design space for COD, BOD_5, and TSS. Contour lines mark 50%, 75%, and 90% removal; black dots denote the six experimental conditions.

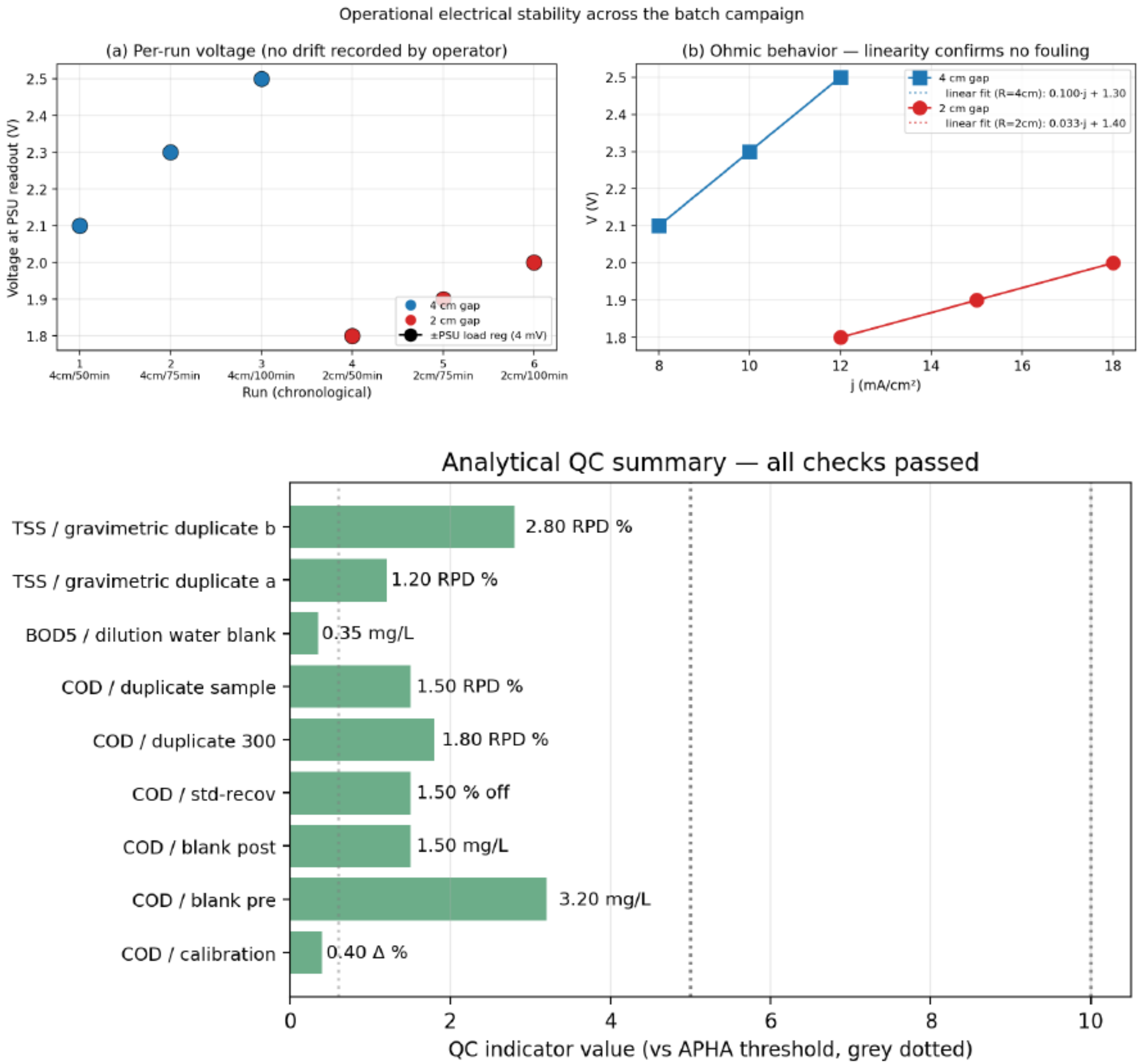

Figure S7 Operational stability evidence. (a) Per-run voltage stability with PSU load-regulation error bars and Ohmic linearity check; (b) QC chart per analyte versus APHA thresholds.

Table S25 Complete full-plant projection (single chamber → 2-EC series → 2-EC + FRP filter). η_{filter} (literature multimedia filter): COD 35%, BOD_5 30%, TSS 70%.

Parameter	Gap	Time (min)	C_{Al} (mg/L)	η single (%)	C_{single} (mg/L)	η 2-EC (%)	C_{2EC} (mg/L)	η full (%)	C_{final} (mg/L)	BM compliance
COD	4 cm	50	102.9	28.9	533	49.5	378.8	67.2	246.2	No
COD	4 cm	75	192.9	44.9	413	69.7	227.4	80.3	147.8	No
COD	4 cm	100	308.7	64.0	270	87.0	97.2	91.6	63.2	**Yes**
COD	2 cm	50	154.4	48.0	390	73.0	202.8	82.4	131.8	No
COD	2 cm	75	289.4	66.7	250	88.9	83.3	92.8	54.2	**Yes**
COD	2 cm	100	463.1	92.7	55	99.5	<5	99.7	<5	**Yes**
BOD_5	4 cm	50	102.9	15.6	270	28.8	227.8	50.2	159.5	No
BOD_5	4 cm	75	192.9	34.4	210	56.9	137.8	69.9	96.5	No
BOD_5	4 cm	100	308.7	59.4	130	83.5	52.8	88.4	37	**Yes**
BOD_5	2 cm	50	154.4	40.6	190	64.7	112.8	75.3	79	No
BOD_5	2 cm	75	289.4	62.5	120	85.9	45	90.2	31.5	**Yes**
BOD_5	2 cm	100	463.1	92.2	25	99.4	2	99.6	<2	**Yes**
TSS	4 cm	50	102.9	1.5	670	2.9	660.1	70.9	198	No
TSS	4 cm	75	192.9	20.6	540	36.9	428.8	81.1	128.6	No
TSS	4 cm	100	308.7	52.9	320	77.9	150.6	93.4	45.2	**Yes**
TSS	2 cm	50	154.4	38.2	420	61.9	259.4	88.6	77.8	No
TSS	2 cm	75	289.4	67.6	220	89.5	71.2	96.9	21.4	**Yes**
TSS	2 cm	100	463.1	97.1	20	99.9	<2.5	100.0	<2.5	**Yes**

Compliance summary: 3/18 at single-chamber; 6/18 after 2-EC series; 9/18 after full plant (2-EC + FRP filter).

Table S26 TEA tornado (cost sensitivity) - complete inputs and outputs. Base case (j^* = 1.5 mA/cm^2; Q = 1 m^3/day; 2 EC chambers + FRP filter): - Tariff: IDR 1,035.78/kWh (PLN industrial 2024) - Al-1100 plate: IDR 40,000/kg (Indonesian market 2024) - Faraday efficiency ϕ: 0.92 - Over-Faradaic factor: 1.30 (Sadaf et al. [3]) - Energy EC: 3.0 kWh/m^3; Balance-of-plant: 0.4 kWh/m^3 - k_{COD} (2 cm): 0.00459 L/mg. Base cost: IDR 21,902/m^3 (USD 1.37/m^3).

Variable (range)	Low (IDR/m^3)	High (IDR/m^3)	Δ abs (IDR/m^3)	Δ% of base
k_{COD} (±30%)	31,047	16,978	14,069	±32.1%
Al price (±30%)	16,390	27,414	11,024	±25.2%
j^* (±20%)	17,634	26,170	8,536	±19.5%
ϕ Faraday (±5%)	23,025	20,886	2,139	±4.9%
Electricity tariff (±30%)	20,889	22,915	2,027	±4.6%

Key insight: Kinetic parameter k is the dominant cost driver (≈±32%), above commodity prices (Al ± 25%, electricity ± 5%). This elevates the kinetic characterization stage from “routine lab work” to high-value TEA input. Variation ranges and their sources are justified in Table S11; this table consolidates the per-parameter cost sensitivity (the former separate tornado breakdown has been merged here).

Correlated Monte Carlo (N = 20,000).

$\phi_{eff} = \phi \cdot (1 - \delta_{passivation})$; δ ~ Beta (2, 18) (mean ≈ 10%); k sampled from bootstrap; j^* solved per draw via Equation 6.

Result: total cost median IDR 21,560 m^{-3} (USD 1.35 m^{-3}); 95% CI IDR 16,800-28,000 m^{-3} (USD 1.05-1.75 m^{-3}). Variance decomposition (squared Pearson contribution, normalised): k 40%, j^* required 30%, C_{Al} 29%, ϕ_{eff} 0.5%, passivation 0.5%, C_{elec} 0.3%.

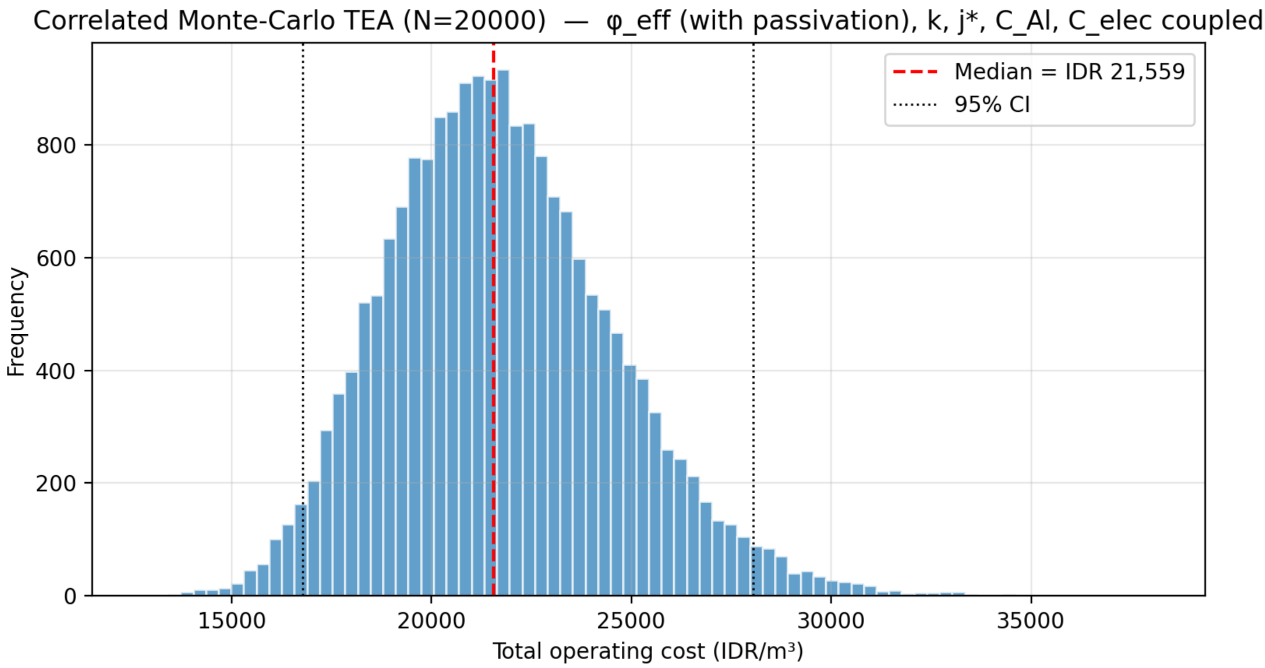

Figure S8 Correlated Monte-Carlo histogram.

Table S27 Carbon footprint comparison with alternative technologies. Emission factors: - Indonesian grid electricity: 0.87 kg CO_2/kWh (PLN 2023) - Primary aluminum: 12 kg CO_2/kg (World Aluminium/IAI 2023) - Recycled aluminum: 1.2 kg CO_2/kg (IAI 2023; 10× lower) - Alum (aluminum sulfate): 1.9 kg CO_2/kg (ecoinvent 3.9) - ZnO (catalyst): ~5 kg CO_2/kg.

Technology	Energy (kWh/m^3)	Chemical input (kg/m^3)	CO_2 energy	CO_2 chemical	CO_2 other	CO_2 total
EC-F this study (primary Al)	3.4	0.77 kg Al	1.13	9.19	0.05	**10.37**
EC-F with recycled Al	3.4	0.77 kg Al (rec.)	1.13	0.92	0.05	**2.10**
EC-F with recycled Al + PV	0.4 (BOP only)	0.77 kg Al (rec.)	0.35	0.92	0.05	**1.32**
Chemical coagulation (alum)	0.3	0.15 kg alum	0.26	0.29	0.05	0.60
Activated sludge (conv.)	0.6	-	0.52	0	0.10	0.62
ZnO photocatalysis	5.0	0.002 kg ZnO	4.35	0.01	0.10	4.46

Interpretation. EC-F with primary Al has the highest CO_2 footprint among the compared technologies (10.4 kg CO_2/m^3), driven by aluminum production (88% of total). Substitution with recycled Al reduces the total to 2.10 kg CO_2/m^3 (~80% reduction). Combined with PV-based power supply, EC-F total drops to 1.32 kg CO_2/m^3, within the same order of magnitude as chemical coagulation and activated sludge while retaining EC's advantages (higher effluent quality, no chemical supply logistics, minimal operator expertise).

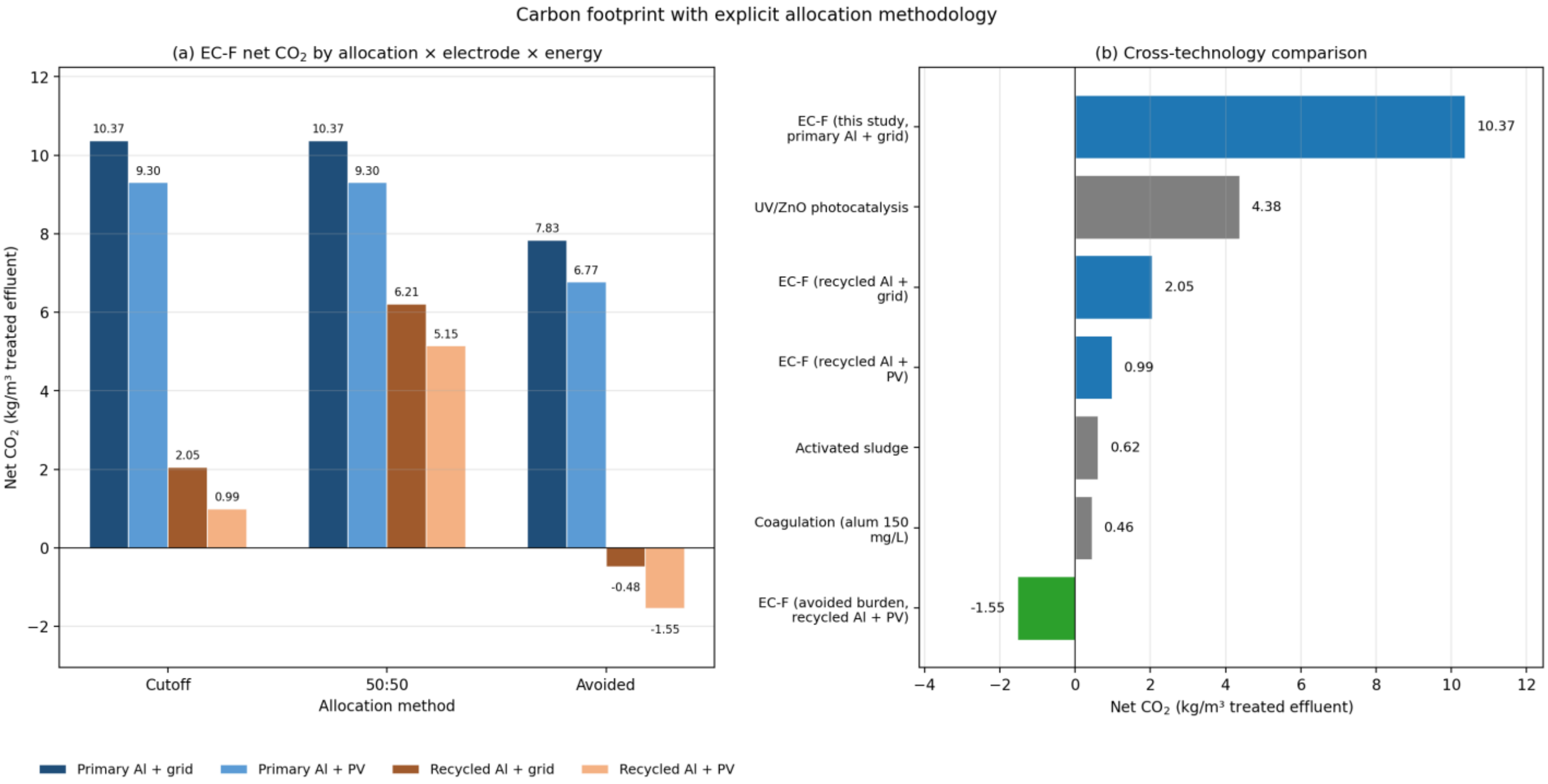

Figure S9 Carbon-footprint scenario matrix. (a) EC-F net CO_2 by allocation × electrode × energy; (b) Cross-technology comparison.

This table extends the main-text Table 8 and adds an explicit caveat on transferability in tabulated form for transparency.

Table S28 Cross-site batik wastewater characteristics (extended).

Reference	Location	Stage	pH	TDS	COD	BOD_5	TSS	Colour (Pt-Co)
This study	Magetan, East Java	Lorod	9.2	3,100	750	320	680	2,000
Kholisoh et al. [13]	Bogor, West Java	Mixed	9.8	2,850	820	350	620	1,850
Indrayani & Rahmah [14]	Yogyakarta	Dye fixation	8.5	-	640	280	540	1,600
Putra et al. [15]	Yogyakarta	Dyeing	9.1	3,200	700	-	720	2,100
Kusumawardani et al. [16]	Indonesia (multi)	Mixed	8-12	2,000-4,000	400-800	160-500	160-700	1,500-5,000
Fadzli et al. [8]	Malaysia	Batik dye	8.9	2,600	580	250	430	1,200

Caveat: Agreement on bulk parameters does not prove kinetic transferability; dye class, conductivity, and trace-ion chemistry are also important. The framework presented should be reparameterised - not transplanted - for clusters with different dye chemistries.

Analytical Code and Raw Data Availability

The analytical code used to produce the statistics, kinetic fits, uncertainty propagation, and figures in this study is available from the corresponding author upon reasonable request. The pipeline - implemented in Python 3.11 with NumPy 2.4, pandas 3.0, SciPy 1.17, statsmodels 0.14, and matplotlib 3.10 - covers triplicate-observation extraction and Faraday dose calculation; Grubbs and Dean-Dixon outlier tests, two-way Type-II ANOVA, Tukey HSD, and non-linear least-squares kinetic fitting with asymptotic Wald confidence intervals; bootstrap confidence intervals for the rate constant *k* (10,000 resamples), exponential-saturation versus Langmuir model selection (AIC/BIC), Holt 1/d IR-limited regime testing, charge-loading analysis, Specific Energy Demand, stoichiometric sludge balance, Monte Carlo uncertainty propagation for j^*, techno-economic tornado sensitivity, and comparative carbon-footprint accounting; and figure generation at 300-600 dpi. The raw instrument source files (experimental design and triplicate observations; Hach DR6000 COD logs; Hanna HI 9146 BOD_5 logs; Sartorius MSA225S TSS logs; laboratory notebook pages; GW Instek PSM-3004 calibration certificate) are likewise available from the corresponding author upon reasonable request.

Source data, figures, and reproducibility scripts for every new SI item are provided in the analysis bundle accompanying this submission.

Reproducibility Note

All new SI computations are reproducible from the analysis bundle accompanying this submission.

References

1. Burnham KP, Anderson DR. Model selection and multimodel inference: A practical information-theoretic approach. New York, NY: Springer; 2002.
2. Holt PK, Barton GW, Mitchell CA. The future for electrocoagulation as a localised water treatment technology. Chemosphere. 2005; 59: 355-367.
3. Sadaf S, Roy H, Fariha A, Rahman TU, Tasnim N, Jahan N, et al. Electrocoagulation-based wastewater treatment process and significance of anode materials for the overall improvement of the process: A critical review. J Water Process Eng. 2024; 62: 105409.
4. Dobrosz-Gómez I, Ibarra-Taquez HN, Gómez-García MÁ. Evaluation of the environmental and economic scope of an electrocoagulation process for the treatment of wastewater from the instant coffee industry. J Solid State Electrochem. 2025; 29: 3441-3463.
5. Hellal MS, Doma HS, Abou-Taleb EM. Techno-economic evaluation of electrocoagulation for cattle slaughterhouse wastewater treatment using aluminum electrodes in batch and continuous experiment. Sustain Environ Res. 2023; 33: 2.
6. Bener S, Bulca Ö, Palas B, Tekin G, Atalay S, Ersöz G. Electrocoagulation process for the treatment of real textile wastewater: Effect of operative conditions on the organic carbon removal and kinetic study. Process Saf Environ Prot. 2019; 129: 47-54.
7. Bazrafshan E, Alipour MR, Mahvi AH. Textile wastewater treatment by application of combined chemical coagulation, electrocoagulation, and adsorption processes. Desalin Water Treat. 2016; 57: 9203-9215.
8. Fadzli J, Puasa SW, Him NR, Hamid KH, Amri N. Electrocoagulation: Removing colour and COD from simulated and actual batik wastewater. Desalin Water Treat. 2024; 320: 100658.
9. Lamhar R, Kambuyi TN, Bejjany B, Kherbeche A, Digua K, Dani A. Electrocoagulation for the decolorization of textile wastewater in single-channel reactor: Response surface methodology for optimization and a novel model exploitation. J Clean Prod. 2024; 450: 141900.
10. Agarwal P, Sangal VK, Mathur S. Treatment of textile effluent by electrocoagulation in a novel reactor to mitigate environmental pollution. Int J Environ Sci Technol. 2025; 22: 3393-3404.
11. Cruz FF, Góes MC, Santana CG, Santos TG, Boscolo M, Luz RC, et al. Optimizing electrocoagulation for textile effluent treatment: Operational efficiency and environmental assessment of Remazol red dye removal. ACS Omega. 2025; 10: 62962-62978.
12. Rezaei S, Heidarpour M, Aghakhani A, Zargoosh K. Comprehensive study on the batch electrocoagulation for real dyeing wastewater treatment. Sci Rep. 2026; 16: 9167.
13. Kholisoh S, Wulandari I, Iryani A, Sutanto S, Warnasih S. Characterization of batik industrial wastewater in Bogor City. Helium. 2022; 2: 20-24.
14. Indrayani L, Rahmah N. Pollutant parameter values as determinants of the treatment-stage effectiveness of batik industry wastewater [Nilai Parameter Kadar Pencemar sebagai Penentu Tingkat Efektivitas Tahapan Pengolahan Limbah Cair Industri Batik] (In Indonesian). J Rek Pros. 2018; 12: 41-50. doi: 10.22146/jrekpros.35754.
15. Putra RS, Annisa AD, Budiarjo S. Batik wastewater treatment using simultaneous process of electrocoagulation and electro-assisted phytoremediation (EAPR). Indones J Chem. 2020; 20: 1221-1229.
16. Kusumawardani SD, Kurnani TB, Astari AJ, Sunardi S. Readiness in implementing green industry standard for SMEs: Case of Indonesia's batik industry. Heliyon. 2024; 10: e36045.